Synthesis, Photophysical Properties, *in Vivo* Photosensitizing Efficacy, and Human Serum Albumin Binding Properties of Some Novel Bacteriochlorins

Ravindra K. Pandey,*[,†] Scott Constantine,[†] Takaaki Tsuchida,[†,‡] Gang Zheng,[†] Craig J. Medforth,[§] Mohamed Aoudia,[||] Andrei N. Kozyrev,[†] Michael A. J. Rodgers,[||] Harubumi Kato,[‡] Kevin M. Smith,[§] and Thomas J. Dougherty[†]

Chemistry Division, Department of Radiation Biology, Division of Radiation Medicine, Roswell Park Cancer Institute, Buffalo, New York 14263, Department of Surgery I, Tokyo Medical College, 6-7-1 Nishishinjuku, Tokyo 160, Japan, Department of Chemistry, University of California, Davis, California 95616, and Center for Photochemical Sciences, Bowling Green State University, Bowling Green, Ohio 43403

Received May 2, 1997[⊗]

The synthesis, photophysical characteristics, *in vivo* photosensitizing efficacy, human serum albumin (HSA) binding properties, and skin phototoxicity of some stable bacteriochlorins were investigated. The novel bacteriochlorins, obtained from chlorophyll-*a*, have long-wavelength absorptions in the range $\lambda_{max} = 734-758$ nm. Preferential migration of ethyl over methyl substituents among ketobacteriochlorins obtained in the pinacol−pinacolone rearrangements of *vic*-dihydroxybacteriochlorins was confirmed by NOE studies. The bacteriochlorins show relatively low fluorescence quantum yields. Among all the bacteriochlorins the triplet states were quenched by ground state molecular oxygen in a relatively similar manner, yielding comparable singlet oxygen quantum yields. In preliminary *in vivo* studies (DBA/2 mice, transplanted with SMT/F tumors), ketobacteriochlorins were found to be more photodynamically active than the related *vic*-dihydroxy analogues. Replacement of the methyl ester functionalities with di-*tert*-butylaspartic acids enhanced the *in vivo* efficacy. Site specific human serum albumin (HSA) binding studies indicated a direct correlation between the ability of the compound to bind to the diazepam binding site (albumin site II) and the *in vivo* photosensitizing efficacy.

Introduction

Some porphyrins and related tetrapyrrolic compounds tend to be retained in malignant tumors at higher concentrations than in normal tissues, thus allowing for the exploitation of this property as a diagnostic tool for the detection and treatment of various types of cancers.[1] The detection of early stage tumors can be accomplished by exposing the porphyrin-containing tumors and the surrounding tissues to light of an appropriate wavelength. The result is that the singlet excited state may then fluoresce, with the response being stronger in those tissues that have retained a higher concentration of the pophyrin than in the surrounding normal tissue. The only sites where this might cause a problem would be in those tissues, such as the liver or the spleen, that also tend to take up and retain porphyrins. In normal epithelial tissue, however, detection can easily be achieved because there is less of a tendency for these tissues to retain porphyrins compared with malignant tissues.[2]

The treatment of cancer by photodynamic therapy (PDT) is based on a similar principle.[3] In brief, the patient is injected with an appropriate dose of a photoactive sensitizing dye. The tumors are then irradiated by light at an appropriate long wavelength absorption. The specific wavelength of light that is delivered activates the dye and results in a tumoricidal effect. It is believed that singlet oxygen is the cytotoxic species and that this together with various oxygen radicals elicit the toxic effects.[4] Among known photosensitizers, Photofrin (a porphyrin derivative) has been studied in most detail and is currently being used all over the world for the treatment of various types of cancers. Despite the fact that it has already been approved for commercialization in Canada, Japan, and the United States, Photofrin has some drawbacks. First of all, it lacks rapid normal tissue clearance, so patients must avoid exposure to sunlight for some significant time following treatment. Also, it is a complex mixture of ether and ester-linked dimers and higher oligomers,[5−8] making it difficult to study mechanistically.[9] Thus, there is a need for further study and development of photosensitizers which may improve upon certain characterisctic of Photofrin.

In recent years, a number of long wavelength (>660 nm) absorbing sensitizers have been reported as potential candidates for achieving maximum tissue penetration.[10,11] Among such compounds, some naturally occurring bacteriochlorins have been reported as effective photosensitizers in preliminary *in vitro* and *in vivo* studies.[12] However, most of the naturally occurring bacteriochlorins which have absorptions at 760−780 nm are extremely sensitive to oxidation, which results in a rapid transformation into the chlorin state which has an absorption maximum at or below 660 nm. Furthermore, if a laser is used to excite the bacteriochlorin *in vivo*, oxidation may result in the formation of a new chromophore absorbing outside the laser window, which reduces the photodynamic efficacy. In order to render PDT more generally applicable to tumor therapy, there is a need for long wavelength absorbing photosensitizers, such as stable bacteriochlorins, which should also

* To whom correspondence should be addressed.
† Roswell Park Cancer Institute.
‡ Tokyo Medical College.
§ University of California.
|| Bowling Green State University.
⊗ Abstract published in *Advance ACS Abstracts,* August 1, 1997.

S0022-2623(97)00289-6 CCC: $14.00

Scheme 1

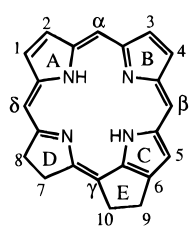

Fischer's system of numbering

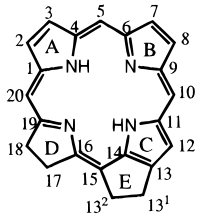

IUPAC System of numbering

be able to localize in relatively high concentration at the tumor site related to normal tissues.

Some time ago, Chang *et al.*[13] showed that chlorins can be converted into *vic*-dihydroxybacteriochlorins upon reaction with osmium tetroxide. We extended this methodology to the pheophorbide-*a* and chlorin e_6 series and prepared a series of *vic*-dihydroxy- and ketobacteriochlorins.[14−17] In our earlier work, we reported that in porphyrin/chlorin systems the regiospecificity of pyrrole subunit modification in the osmium tetroxide oxidation is affected significantly by the presence of the electron-withdrawing/donating groups on the periphery of the macrocycle.[14,18] Stable ketobacteriochlorins prepared from the corresponding *vic*-dihydroxymesochlorin e_6 trimethyl ester, methyl *vic*-dihydroxymesopyropheophorbide-*a*, and related 2-formyl analogues had strong absorptions in the region 710−760 nm region but did not show any photosensitizing activity in mice (DBA/2) transplanted with SMT-F tumors.[19]

The main focus of our current research has been concentrated on (i) synthesis of photosensitizers with absorption maxima near or above 700 nm and (ii) understanding their mechanistic transport and *in vivo* binding properties.[20] In general, protein binding accounts for the transport of a very large proportion of systemically injected porphyrins and their analogues. The affinity of serum albumin and serum lipoproteins for porphyrins indicates a potential role for these proteins as endogenous carriers for porphyrins in PDT.[21] As a drug carrier, a protein may aid in the selective delivery of the porphyrin to a tumor region, and lipoproteins may facilitate drug access into the cell via receptor mechanisms. It has also been shown that the distribution of porphyrins among serum proteins is dependent upon their chemical structure. X-ray diffraction has shown that HSA mainly consists of two binding sites (site I and site II).[22] The conformations of these sites are similar, but the binding residues are different (site I, Lys-His; site II, Arg-Tyr). There are a few reports in which the HSA binding affinity of Photofrin has been studied, although unfortunately due to the complex chemical nature of Photofrin these binding studies were inconclusive. Recently, in our studies on a series of alkyl ether analogues of pyropheophorbide-*a*,[23] we observed a direct correlation of *in vivo* photosensitizing activity with the ability of the compound to bind to albumin site II (Tsuchida et al., manuscript in preparation). This study was then extended to a series of regiochemically pure components of Photofrin, and similar results were obtained.[24]

In the present study, we synthesized a series of stable ketobacteriochlorins and *vic*-dihydroxybacteriochlorins from methyl 9-deoxy-2-devinyl-2-ethylpyropheophorbide-*a*. These compounds are then evaluated in terms of their *in vivo* efficacy, skin phototoxicity, photophysical properties, and site specific albumin binding ability.

Results and Discussion

Chemistry. The numbering system for tetrapyrroles approved by IUPAC−IUB has been used and is shown in Scheme 1. For the preparation of desired bacteriochlorins, methyl pheophorbide-*a*, **1**, extracted from *Spirulina pacifica* alga, was used as a starting material.[25] Pyrolysis of **1** with 2,4,6-collidine gave methyl pyropheophorbide-*a*, **2**,[26] which upon reaction with $NaBH_4$/TFA[27] produced 13^1-deoxypyropheophorbide-*a* (**3**) in 80% yield (Scheme 2). The corresponding Ni(II) complex **4** was obtained in quantitative yield by refluxing **3** with nickel acetylacetonate [Ni($acac_2$)] in *o*-xylene,

Scheme 2

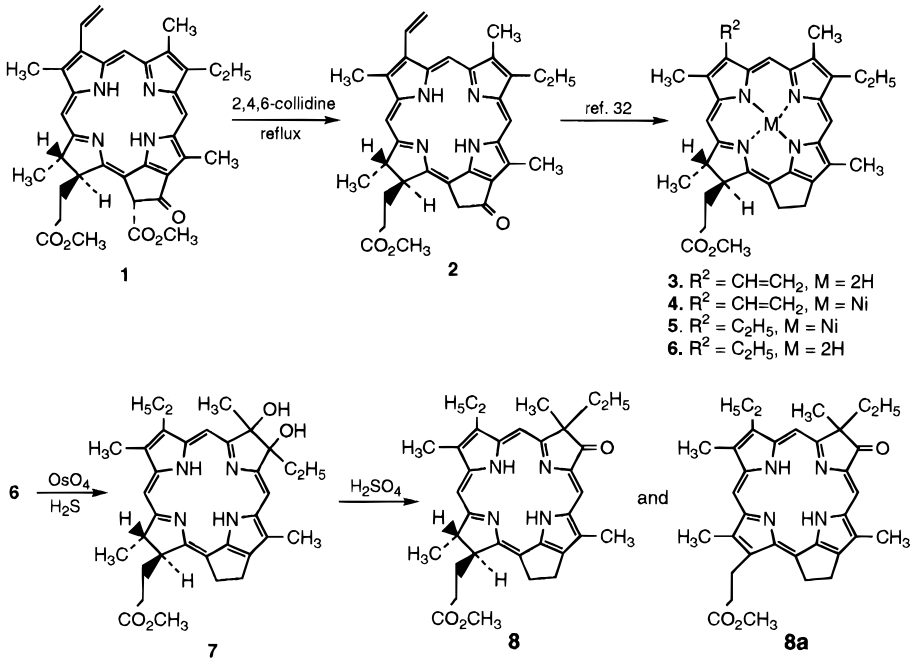

Scheme 3

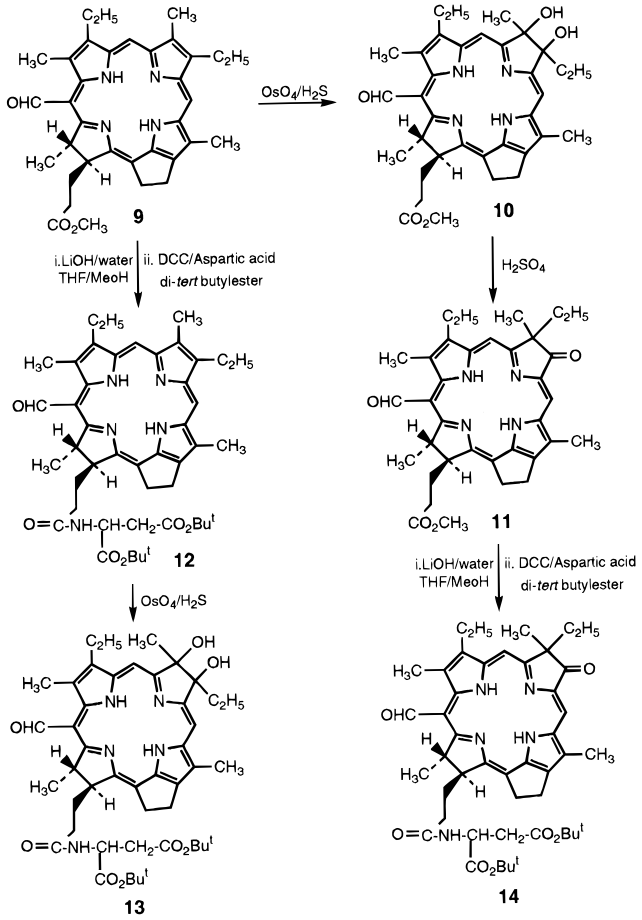

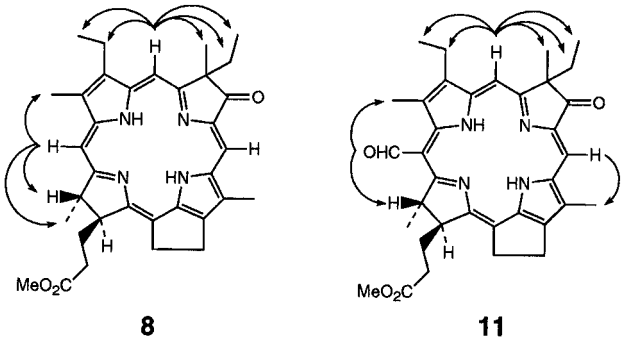

8 **11**

Figure 1. NOE assignments for bacteriochlorins **8** and **11**.

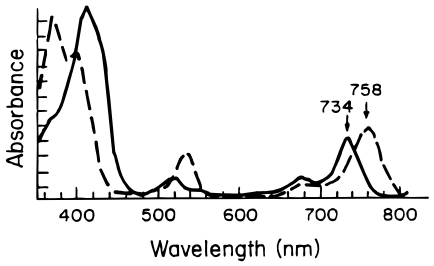

Figure 2. Optical spectra of bacteriochlorins **13** (—) and **14** (- - -) (in CH_2Cl_2).

Table 1. Absorption Maxima (Q Band), Fluorescence Emission Maxima, and Fluorescence Quantum Yields (Φ_f) in Benzene

compd	λ_{max} (absorption)/nm	λ_{max} (fluorescence)/nm	Φ_f
10	757	686 and 768	0.002
11	734	686 and 750	0.002
13	753	687 and 760	0.002
14	734	693 and 750	0.004

which upon hydrogenation gave methyl 13[1]-deoxymesopyropheophorbide-*a* (**5**) in >90% yield. Demetalation was achieved by stirring **5** in concentrated H_2SO_4 for 30 min, and the related free base derivative **6** was isolated in 98% yield after diazomethane treatment. Reaction of **6** with osmium tetroxide/pyridine/H_2S afforded *vic*-dihydroxybacteriochlorin **7** in 65% yield, which under pinacol−pinacolone reaction conditions (treatment with concentrated H_2SO_4) gave a mixture of ketobacteriochlorin **8** and chlorin **6**. Leaving the ketobacteriochlorins **8** at room temperature for an extended period gave **8a**. The structure of **8a** was confirmed by single X-ray crystal studies (Senge and Pandey, unpublished results). Treatment of 20-formyl-*vic*-dihydroxybacteriochlorin **10** analogue under similar pinacol−pinacolone reaction conditions afforded ketobacteriochlorin **11** as the sole product. These results suggest that the presence of an electron-withdrawing group such as CHO, at positions adjacent to of the reduced pyrrole ring (ring D), inhibits oxidation of this ring.

For the preparation of *vic*-dihydroxybacteriochlorin **13**, the methyl ester **10** was hydrolyzed to carboxylic acid, which on reacting with DCC and aspartic acid di-*tert*-butyl ester gave the desired product in 80% yield (Scheme 3). By following a similar approach ketobacteriochlorin **11** was converted to ketobacteriochlorin **14** in 75% yield. The structures of all the new compounds were confirmed by ^1H NMR and high-resolution mass spectroscopy (HRMS). The *vic*-dihydroxy compounds **10** and **13** were obtained as diasteriomeric mixtures in which the *vic*-hydroxy groups were up or down relative to ring D. Preferential migration of the ethyl over the methyl group in ketobacteriochlorns **8** and **11** was confirmed by NOE studies (Figure 1).

The progress of reactions at all stages was monitored by spectrophotometry. For example, pyropheophorbide-*a* (**2**) has long wavelength absorption at 658 nm. Reduction of the 13[1]-C=O to CH_2 produced methyl 9-deoxypyropheophorbide-*a* (**6**) with a long wavelength absorption maximum at 646 nm. Introduction of a CHO group at the δ-meso position of pheophorbide **9** produced a significant bathochromic shift and a strong absorption at 678 nm. Reaction of formylchlorin (**9**) with OsO_4 and reductive cleavage of the osmate ester with H_2S afforded *vic*-dihydroxybacteriochlorin (**10**) (λ_{max} 760 nm). Compared to diols **10** and **13**, the related ketobacteriochlorins **8** and **14** showed hypsochromic shifts and had long wavelength absorption with λ_{max} at 734 nm (Figure 2).

Photophysical Properties. All compounds have the common bacteriochlorin structure and differ only by their peripheral substitution at C-7, C-8, C-17, and C-20 (see Scheme 1). The *vic*-dihydroxybacteriochlorins have two hydroxyl groups at the C-7 and C-8 positions, whereas the corresponding ketobacteriochlorin analogues possess a carbonyl group at position C-8. These structural differences are reflected in absorption and fluorescence spectral shift (Table 1). For example the presence of the carbonyl group in compound **14** induces a shift of the long Q-band to a lower wavelength. A similar shift was observed in the fluorescence spectrum. Thus, it appears that nonconjugated exo substituents such as OH have no effect upon optical spectra, and somewhat stronger effects are observed with conjugated but "dead end" substituents, such as the carbonyl group.

Table 2. Triplet Decay Rate Constant in Argon-Saturated Solutions (K_0), Triplet Absorption Maxima (λ^T_{max}), Triplet Quenching Rate Constant by Oxygen (K_q), and Singlet Oxygen Quantum Yields (Φ_Δ)

compd	$10^{-4}K_0$/ s^{-1} [a]	λ^T_{max}/ nm	K_q/ $10_9\ M^{-1}\ s^{-1}$	$\Phi_\Delta \pm 0.05$
10	757	686 and 768	0.002	0.46
11	734	686 and 750	0.002	0.35
13	753	687 and 760	0.002	0.40
14	734	693 and 750	0.004	0.41

[a] Error limits ± 5%.

This effect may be attributed to changes in electron density in the ring induced by the conjugated π bond of the carbonyl group. It is interesting to note that both compounds show relatively low fluorescence quantum yields, Φ_f (Table 1).

The properties of the triplet state indicate that the presence of the hydroxyl groups tends to reduce the triplet state lifetime, irrespective of the nature of the substituents in position C-17 (Table 2). However, all triplet states are quenched by ground state molecular oxygen in a relatively similar manner, yielding comparable singlet oxygen quantum yields within the experimental errors (Table 2). General methods for photophysical characterizations are discussed in the Experimental Section.

Human Serum Albumin Binding Studies. Human serum albumin (HSA) is one of the key compounds in human blood that affect many drug distributions. Several binding sites in HSA were recognized using replacement methodology with fluorimetry by Sudlow *et al.*[28,29] In their studies, two major binding sites of HSA were recognized. The site binding with 5-(dimethylamino)naphthalene-1-sulfonamide (DNSA) was named site I, and the site binding with dansyl-L-proline (DP) was named site II. It has been shown that HSA has three major domains, each with two subdomains. Major binding sites, namely site I and site II, are located at subdomain IIA and IIIA, respectively.[22] Focal points of the binding sites are a positively charged residue, such as lysine or arginine, and a ring-formed polarized residue such as tyrosine or histidine. In the case of site I of HSA, a focal point was found to be Lys 199 and His 242.[22] In the case of site II of HSA, it was Arg 410 and Tyr 411.[22]

A decrease in the fluorescence intensity of the complex (probe/HSA) with drugs can be interpreted as a displacement of the probe from its binding site by the addition of drug through a competitive mechanism or an allosteric mechanism. In the case of allosteric displacement, the fluorescence spectrum of the probe, DNSA or DP, should shift to longer wavelength while the intensity is decreased. Thus, if the fluorescence spectrum of the probe does not shift, the fluorescent probe and the drug might have the same binding site. Therefore, this technique is often employed to characterize the binding sites of various drugs. The displacement of the probes by a drug, which has no intrinsic fluorescence at the excitation wavelength, was monitored by measuring the resultant evolution in the probe fluorescent intensity.

Binding properties of bacteriochlorin derivatives **10**, **11**, **13**, and **14** with site I and site II were obtained by the NLSCF technique. Simulation curves for ketobacteriochlorins **11** and **14** with each site I and site II

Table 3. HSA Binding Affinity of Bacteriochlorins

compd	displacement of DP[a]	binding constant (L/mol)[b] site I	site II
10	−	5×10^5	
11	+	5×10^5	5×10^5
13	−	5×10^5	
14	+	5×10^5	5×10^5

[a] Determined by ultrafiltration method. [b] Estimated from titration of HSA/sensitizer complex with fluorescent probes.

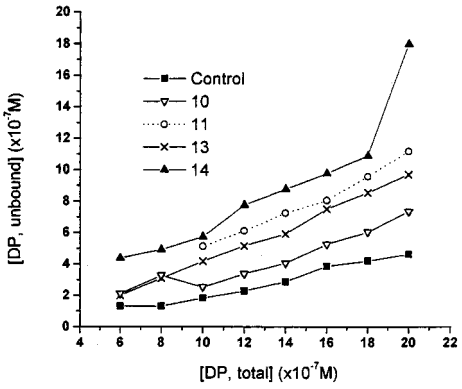

Figure 3. Displacement of site II (HSA) specific probe (densylproline) with bacteriochlorins **10**−**14** by performing filtration experiments.

appears to fit a model which consists of both competitive and independent binding sites. The result of the NLSCF analysis for ketobacteriochlorin **10**, **11**, **13**, and **14** are shown in Table 3. These results indicated that all bacteriochlorins bind with site I on HSA. Unlike bacteriochlorins **10** and **13**, when bacteriochlorins **11** and **14** were used as substrates the displacement of DP from site II was also observed. These results suggest that ketobacteriochlorins **11** and **14** bind with site I and site II of HSA, while the dihydroxybacteriochlorins **10** and **13** showed preferential site I HSA binding affinity. The results are summarized in Table 3.

To further confirm the results obtained by fluorometric titration experiments, an ultrafiltration experiment was performed.[24] Unlike the titration method which measures the fluorescence intensity based on bound probe, the ultrafiltration method measures the fluorescence intensity of unbound probe by adding a large amount of HSA. The results obtained from bacteriochlorins **10**, **11**, **13**, and **14** are summarized in Figure 3.

In order to establish a general relationship of *in vivo* PDT efficacy of various types of photosensitizers with binding sites of HSA, bacteriochlorins **10**, **11**, **13**, and **14** with variable hydrophilic/hydrophobic characteristics were investigated for *in vivo* photosensitizing efficacy. Among these photosensitizers, the keto derivatives **11** and **14** were found to be more effective than the related *vic*-dihydroxy derivatives **10** and **13**. However, the best *in vivo* PDT efficacy was observed for ketobacteriochlorin **14** in which the methyl ester functionality was replaced with an aspartyl group.

From these results it seems that there is a direct correlation of *in vivo* photosensitizing activity with the ability of the compound to bind to site II of HSA. Since it seems unlikely that the site II binding is significant *per se*, one possible explanation is that there may be a specific cellular site with similar steric and electronic requirements (e.g. diazapam binding sites). It has been

Table 4. Preliminary *in Vivo* Photosensitizing Efficacy in DBA/2 Mice Transplanted with SMT/F Tumors[a,b]

compd	dose (mg/kg)	λ_{max} (nm)[c]	time (h), postinj	% response (days)[d]					
				1−5	6−10	11−15	16−20	21−25	26−30
10	5.0	763	3.0	no response					
11	5.0	739	3.0	100	60[e]	60	0		
	2.5	739	3.0	100	100	80	60	60	20
	1.0	739	3.0	no response					
13	5.0	763	3.0	100	100	100	80	50	50
	5.0	763	24.0	no response					
	2.5	763	3.0	no response					
14	5.0	739	3.0	100% mortality on day 1					
	5.0	739	24.0	no response					
	2.5	739	3.0	100	100[f]	60	60	60	60
	1.0	739	3.0	100	80	60	60	50	50
Photofrin	5.0	630	24	100	100	80	60	50	50

[a] Nonpalpable tumors. [b] Under similar treatment conditions, the drug alone or light without drug did not show any antitumor activity. [c] Determined by *in vivo* reflection spectroscopy. [d] 75−80 mW/cm^2, ~135 J/cm^2, six mice/group. [e] 33% mortality by day 6. [f] 50% mortality by day 7, percentages shown are based on the basis of survived mice (mice used: six mice/group).

shown that cytochrome *c* oxidase is one of the target proteins in PDT.[30] This protein is located on the inner membrane of mitochondria. In order to target this protein, photosensitizers have to pass through the outer membrane of mitochondria. The mitochondrial benzodiazepine receptor is believed to act as a "gate" on the outer membrane for porphyrins.[31] While site II is known as a benzodiazepine binding site on HSA, the mitochondrial benzodiazepine receptor might have a structure similar to that of site II. Thus, photosensitizers which do not bind to site II may not pass through the outer membrane of the mitochondria. Therefore, the sensitizers would be unable to target cytochrome c oxidase. Further studies to investigate our hypothesis are currently in progress. The mathematical equations used for determing the binding constants of various photosensitizers are discussed in the Experimental Section.

***In Vivo* Biological Studies.** Prior to *in vivo* biological evaluation, the purity of new sensitizers was ascertained by HPLC, and they were then dissolved in 1% Tween 80/water to provide an injectable solution. The concentration of the sensitizers were calculated (diluted with freshly distilled THF for disaggregation) on the basis of their extinction coefficient (ϵ) values, which were measured in dichloromethane solutions.

(a) Tumor Response. In order to evaluate new photosensitizers for *in vivo* efficacy, a 1 mm piece of SMT-F tumor removed from a donor DBA/2 HA-DD mouse was implanted subcutaneously with a trocar into the axilla of the 5−7-week-old female DBA/2 HA-DD mice. When tumors grew to about 5 mm diameter, mice were injected (iv) with photosensitizers at various doses. At variable times after injection, mice were restrained in aluminum holders, and each tumor was illuminated with 135 J/cm^2 light from a laser tuned at the longest wavelength absorption maximum of the particular photosensitizer. The amount of sensitizer initially injected was intentionally kept high in order to determine the biological effectiveness of these compounds. If the compound showed some activity, the amount of drug and the time of treatment were varied and optimum treatment conditions were determined. The shifts in *in vivo* absorptions of new bacteriochlorins were determined by *in vivo* reflectance spectroscopy. Comparing to *in vitro* absorptions, these compounds exhibit a red shift of about 5 nm in their *in vivo* electronic absorption spectra, so the mice (transplanted with SMT/F tumors) were treated at those particular wavelengths.

The *in vivo* results are summarized in Table 4. In brief, bacteriochlorin **13** at dose of 5 mg/kg showed photosensitizing ability when the mice were treated 3 h postinjection of the drug at 763 nm (*in vivo* absorption). However, at the same dose, when the treatment was done at 24 h postinjection, no tumor response was observed. Bacteriochlorin **10**, which is structurally similar to diol **13**, except that the aspartic acid di-*tert*-butyl ester side chain at position 17 has been replaced by a methyl ester, did not show any activity at similar treatment conditions. Bacteriochlorin **14** in which a keto (C═O) group was regioselectively introduced at position 8 of the macrocycle (ring B) showed extreme toxicity at a dose of 5.0 mg/kg, and 100% mortality was observed after the light treatment. This result suggests that compound **14** is either extremely potent or highly toxic. The experiment was therefore repeated at a lower dose (2.5 mg/kg, six mice/group) by treating at 3 h postinjection. Interestingly, a 100% tumor response was observed on day 7. However, three out of six mice had died. The responses of the surviving mice were followed until day 30, and all surviving mice were tumor free. Conversely, at the same light and drug doses the mice treated 24 h postinjection of the drug did not demonstrate any tumor cure. These results indicate that ketobacteriochlorin **14** tends to clear rapidly from the tumors. Further reducing the dose to 1.0 mg/kg and treating 3 h postinjection at 739 nm resulted in 100% tumor cure on the following day without any mortality, and at day 30, >50% of the mice (7/12 mice) were tumor free. Under similar treatment conditions bacteriochlorin **11** did not show any tumor response. From these results it can be concluded that the presence of various hydrophilic or hydrophobic substituents make a significant difference in tumor localizing efficacy. For example, the presence of methyl ester functionalities in **10** and **11** make the photosensitzer more hydrophilic due to their *in vivo* conversion into the corresponding carboxylic acids by the enzyme esterases and, thus, probably do not retain in tumors for longer time. The butyl ester groups in photosensitizers **13** and **14** would most certainly take a longer time to hydrolyze by the enzyme and thus would be retained in tumors for a longer time. Compared with diol **13**, the keto derivative **14** is more hydrophobic and also showed better *in vivo* efficacy.

(b) Normal Tissue Response. Since the prolonged cutaneous phototoxicity is a potential serious side effect of Photofrin administration, we compared the photo-

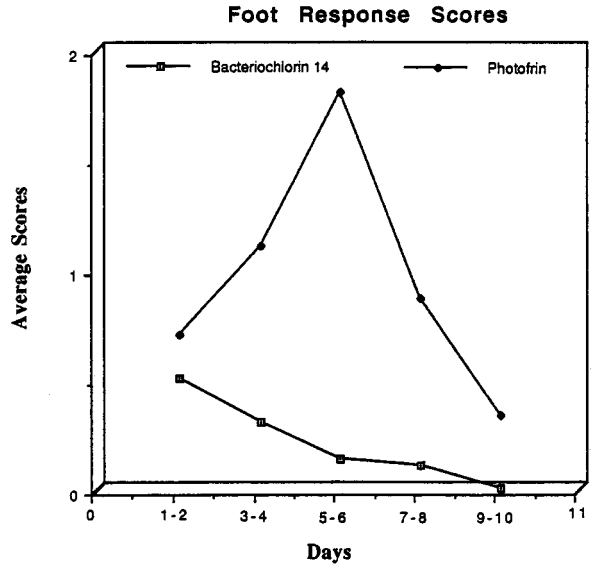

Figure 4. Comparative skin phototoxicity (at equivalent tumor therapeutic doses) of bacteriochlorin **14** (1.0 mg/kg) with Photofrin (5.0 mg/kg) in DBA/2 mice. (0,0) no reaction; (0,3) slight edema; (0,5) moderate edema; (0,8) moderate erythema; (1,1) large edema with erythema/slight epilation; (1,4) slight epilation with moderate edema and/or erythema; (1,8) slight desquamation and epilation; (2,0) moderate dry desquamation and swelling of toes; (2,4) slight moist desquamation.

toxicity of ketobacteriochlorin **14** (which showed the best tumor cure) with that of Photofrin. The foot response experiments were carried out on 5−7-week-old Swiss mice. Photosensitizer **14** was injected at a dose of 1.0 mg/kg (the therapeutic dose) in 1% Tween 80/water. The skin phototoxicity of these sensitizers was compared with that of Photofrin at a dose of 5.0 mg/kg. Approximately 24 h postinjection, the mice were restrained without anesthesia in aluminum holders, and one hind foot of each mouse was illuminated with light from an argon-pumped dye laser at its maximum long wavelength absorption. The light dose rate was measured with coherent 210 power meter; wavelength was determined with a PTR Optics monochromator. As can be seen from Figure 4, bacteriochlorin **14** cleared from the tissue very rapidly and at day 9 no significant phototoxicity was observed. Under a similar experiment, Photofrin showed considerable skin phototoxicity.

Experimental Section

Chemistry. Melting points are uncorrected and were measured on a Fischer/Johns microscopic hot stage apparatus. Electronic absorption spectra were measured on a Spectrotonic Genesys 5 spectrophotometer using solutions in dichloromethane. Mass spectra were obtained at the Mass Spectrometric Facility, Department of Biophysics, Roswell Park Cancer Institute, Buffalo, NY, on a VG Analytical ZAB-HS-2F mass spectrometer using a direct insertion probe. EI spectra were acquired at 70 eV, 50 mA, and a source temperature of 200 °C. ^{1}H-NMR spectra were obtained using a General Electric QE-300 spectrometer. Samples were dissolved in $CDCl_3$, and chemical shifts are reported relative to $CHCl_3$ at 7.258 ppm. Reactions were monitored spectrophotometrically and by analytical thin-layer chromatography on cut strips (ca. 2 cm × 6 cm) of Kodak 13179 silica gel (0.25 mm thickness) plastic-backed sheets. Preparative TLC was conducted on 20 cm × 20 cm glass plates coated with ca. 1 mm thick Analtech silica gel GF. For column chromatography two types of packings were used: (i) Alumina (70−230 mesh) was deactivated with 6% H_2O (Brockmann grade III) before use. (ii) Silica gel 60 (70−230 mesh) was used for normal gravity chromatography. Analytical HPLC was performed using a Spectra Physics SP8700 solvent delivery system equipped with a Rheodyne injector, and a Spectroflow 757 programmable multiwavelength detector was set either at 405 nm or at the long wavelength absorption maxima of the compounds. The separation profiles were recorded using a Spectra Physics 4270 integrator. Reverse phase separations were carried out using a Merck LiChroCart 250-4 RP-8 (5 μm) column, using water/MeoH as eluant; solvent A is 400 mL of distilled H_2O and 600 mL of MeOH, the solution is then buffered to a pH of 7.5 with H_3PO_4. Solvent B consists of 100 mL of distilled H_2O and 900 mL of MeOH, also buffered to pH = 7.5. The solvents were degassed by purging for approximately 1−2 min under a heavy flow of helium, and were then kept under the same atmosphere. Samples were filtered through a 0.45 μm filter prior to injection. The gradient program used in this study began initially with solvent A and gradually changed over to the more polar solvent system B within 40 min (flow rate, 1.5 mL/min). Solvent B was then run for 10 min at the same flow rate before switching over to solvent A (10 min). For performing various reactions, tetrahydrofuran (THF) was distilled over sodium metal and dichloromethane was distilled over calcium hydride.

Methyl 13^1-Deoxymethylpyropheophorbide-*a* (3). Methyl pyropheophorbide-*a* (**2**) (1.5 g) was dissolved in methylene chloride (250 mL), trifluoroacetic acid (125 ml) was added, and the reaction mixture was stirred at 0−5 °C for 10 min. Sodium borohydride (3.5 g) was added slowly within 30 min. The reaction mixture was then stirred at room temperature and was monitored spectrophotometrically. It was then diluted with dichloromethane (250 mL) and slowly poured into water. The dichloromethane extract was washed with water (3 × 200 mL), aqueous sodium bicarbonate (until the solution pH was neutral), and again with water. The organic layer was separated and dried over anhydrous sodium sulfate. Evaporation of the solvent gave a residue, which was chromatographed on a neutral (grade III) alumina column. The solvent was evaporated, and the residue was crystallized from CH_2Cl_2/hexane in 80% yield (1.17 g): mp 180−182 °C (lit.[32] mp 179−180 °C); ^{1}H NMR δ 9.48, 9.40, and 8.56 (each s, 1H, meso H), 8.00 (dd, 1H, C*H*=CH_2), 6.17−6.30 (m, 2H, CH=C*H*$_2$), 4.80 to 5.10 (m, 4H, 13^1,15^1-CH_2CH_2), 4.50 (m, 1H, 18-H), 4.28 (m, 1H, 17-H), 3.70 (m, 4H, 2 C*H*$_2$CH$_3$), 3.62 (s, 3H, CO_2CH_3), 3.32 (s, 6H, 2 ring CH_3), 3.16 (s, 3H, ring CH_3), 2.85−2.50 (m, 4H, 17-$CH_2CH_2CO_2CH_3$), 1.68 (t, 6H, 2 × CH_2CH_3), 1.52 (d, 3H, 18-CH_3).

Nickel(II) Methyl 13^1-Deoxymesopyropheophorbide-*a* (5). Methyl 13^1-deoxypyropheophorbide-*a* (**3**) (1.0 g) was converted into its nickel complex **4** by reacting with nickel acetylacetonate in refluxing o-xylene for 1.5 h. After the standard workup, the crude residue was chromatographed on a neutral alumina (Gr III) column. The appropriate eluates were combined. The residue obtained after evaporating the solvent was redissolved in THF and hydrogenated in presence of 10% Pd/C. The solvent was evaporated, and the residue was crystallized from methylene chloride/hexane in quantitative yield (1.1 g): mp 220−225 °C; ^{1}H NMR δ 9.44, 9.35, and 8.30 (each s, 1H, meso H), 4.82−5.18 (m, 4H, 13^1,15^1-CH_2CH_2), 4.42 (m, 1H, 18-H), 4.24 (m, 1H, 17-H), 3.72 (m, 4H, 2 C*H*$_2$CH$_3$), 3.65 (s, 3H, CO_2CH_3), 3.30 (s, 6H, 2 ring CH_3), 3.18 (s, 3H, ring CH_3), 2.8−2.30 (m, 4H, 17-CH_2CH_2), 1.70 (t, 6H, 2 × CH_2CH_3), 1.50 (d, 3H, 18-CH_3); HRMS calcd for $C_{34}H_{38}N_4O_2$-Ni 592.2343, found 592.2340.

Methyl 13^1-Deoxy-20-formylmesopyropheophorbide-*a* (9). Vilsmeier reagent prepared from dimethylformamide (5.0 mL) and phosphorous oxychloride (4.0 mL) was reacted with pheophorbide-*a* (**4**) (700 mg) dissolved in methylene chloride (100 mL) at 0−5 °C for 1h and then at room temperature for 4 h, under nitrogen atmosphere. The reaction mixture was diluted with methylene chloride (200 mL). A saturated solution of sodium bicarbonate was added until the pH was ~12. The reaction mixture was stirred at room temperature overnight, extracted with methylene chloride (3 × 200 ml), and washed with water. The organic layer was separated, dried over anhydrous sodium sulfate, and evaporated. The crude product was chromatographed over an alumina (grade III)

column, eluting with methylene chloride. The major band was collected. Evaporation of the solvent gave a residue which was treated with 10% H_2SO_4/TFA (v/v, 50 mL) for 2 h. It was poured into water, extracted with methylene chloride, washed with aqueous sodium bicarbonate, and then washed again with water. The organic layer was separated and dried over anhydrous sodium sulfate. Evaporation of the solvent gave the title compound, which was crystallized from CH_2Cl_2/hexane in 75% yield (500 mg): mp 230−231 °C; UV−vis λ_{max} (nm, ϵ) 408 (102 800), 514 (6300), 546 (6500), 627 (4800), 678 (16 400); ^{1}H NMR δ (ppm) 12.00 (s, 1H, CHO), 9.70, 9.30 (each s, 1H, meso H), 5.30 (t, 2H, CH_2 (ring E)), 4.12 (m, 3H, CH_2 (ring E), and 18-H), 4.20 (m, 1H, 17-H), 3.90 and 3.70 (each m, 4H, 2 × CH_2CH$_3$), 3.60 (s, 3H, CO_2CH_3), 3.40, 3.38 (each s, 3H, ring CH_3), 2.82−2.48 (m, 4H, 17-CH_2CH_2), 1.70 (t, 6H, 2 × CH_2CH_3), 1.40 (d, 3H, 18-CH_3), −1.52 (s, 2H, 2NH); HRMS calcd for $C_{39}H_{40}N_4O_3$ 564.3094, found 564.3101.

13^1-Deoxy-20-formylmesopyropheophorbide-*a* Di-*tert*-butyl Aspartate (12). The chlorin **9** (150 mg) was dissolved in THF (5 mL). Methanol (15 mL) and lithium hydroxide (250 mg) dissolved in distilled water (15 mL) were added. The reaction mixture was stirred at room temperature under nitrogen atmosphere overnight and was monitored by analytical TLC. Chloroform (200 mL) was added, and the aqueous layer was separated. The pH was adjusted to 5.0 using 2% aqueous HCl. The mixture was then extracted with methylene chloride (2 × 200 mL). After the standard workup as discussed for the foregoing compounds, the residue was crystallized from methylene chloride/hexane as a fine powder in quantitative yield. It was redissolved in methylene chloride, and DCC (150 mg), DMAP (10 mg), and aspartic acid di-*tert*-butyl ester (150 mg) were then added. The reaction mixture was stirred at room temperature overnight. It was then filtered, and the residue obtained after evaporating the solvent was chromatographed over a alumina column (grade III). The major product obtained after evaporating the solvent was purified by preparative silica plates, eluting with 2% methanol/methylene chloride. Evaporation of the solvent gave a residue, which was crystallized from $CHCl_2$/hexane in 80% yield (165 mg): mp 242−245 °C dec; UV−vis [λ_{max} (nm), ϵ] 410 (103 800), 514 (6200), 545 (6600), 627 (4800), 678 (17 000); ^{1}H NMR δ 12.00 (s, 1H, CHO), 9.70, 9.28 (each s, 1H, 2 meso H), 6.42 (1H, CONH), 5.30−3.65 (total 12H, 13^1,15^1-CH_2CH_2, 17-H, 18-H, 2 × CH_2CH$_3$, CHCO$_2$Bu^t, CH_2CO$_2$Bu^t), 3.70 and 3.65 (each s, 3H, ring CH_3), 2.0−2.80 (m, 4H, 17-CH_2CH_2), 1.85 (s, 3H, 8-CH_3), 1.70 (t, 3H, CH_2CH_3), 1.45 [12H, 18-CH_3 and $CO_2C(CH_3)_3$], 1.25 [s, 9H, $CO_2C(CH_3)_3$], 0.50 (t, 3H, 8-CH_2CH_3), −0.40 and −1.70 (each s, 1H, NH); HRMS calcd for $C_{46}H_{59}N_5O_6$ 777.4458, found 777.4560.

Methyl 13^1-Deoxy-8-ketobacteriochlorin (8). 13^1-Deoxypheophorbide **6** (200 mg) was dissolved in dichloromethane (20 mL). Pyridine (5 drops) and osmium tetroxide (200 mg)/diethyl ether (2.0 mL) were added. The reaction mixture was stirred in a sealed flask overnight and was monitored by analytical TLC and spectrophotometrically. It was diluted with methylene chloride (50 mL), H_2S gas was bubbled through the solution for 5 min, and the solution was filtered. The filtrate was evaporated, and the residue was chromatographed over silica column, eluting with 5% methanol/methylene chloride. The slow-moving band was collected. After the solvent was evaporated, the corresponding diol **7** was crystallized from CH_2Cl_2/hexane as a fluffy solid. The intermediate **7** was reacted with H_2SO_4 (10 mL) for 20 min, poured into ice cold water, and extracted with dichloromethane. The dichloromethane layer was washed with aqueous sodium bicarbonate and finally with water. The organic layer was then dried over anhydrous sodium sulfate, and the solvent was evaporated. The residue was found to be a mixture of mainly two compounds by analytical TLC; the faster moving band was characterized as 13^1-deoxymesopyropheophorbide-*a* (**6**) and a slower moving band was identified as the desired bacteriochlorin **8**.

Chlorin 6: mp 246−248 °C; UV−vis λ_{max} (nm, ϵ) 396 (135 800), 498 (9500), 585 (6400), 618 (7800), 639 (30 250); ^{1}H NMR δ (ppm) 9.85, 9.60, 8.80 (each s, 1H, meso H), 5.80 and 4.95 (each m, 2H, 13^1,15^1-CH_2CH_2), 5.20 and 4.50 (each m, 1H, 17-H and 18-H), 4.10 (q, 4H, 2 × CH_2CH_3); 3.72, 3.68, 3.60, and 3.58 (each s, 3H, CO_2CH_3 and ring CH_3), 2.75−2.20 (m, total 4H, 17-CH_2CH_2), 1.90 (d, 3H, 18-CH_3), 1.80 (t, 6H, 2 × CH_2CH_3), −0.5 and −1.7 (each broad s, 1H, NH); ^{1}HRMS calcd for $C_{34}H_{40}N_4O_2$ 536:7156, found 536.7150.

Ketobacteriochlorin 8: mp 250 °C dec; UV−vis λ_{max} (nm, ϵ) 417 (112 000), 501 (8400), 543 (4900), 636 (6400), 684 (50 400); ^{1}H NMR δ (ppm) 9.81, 8.77, and 8.71 (each s, 1H, meso H), 5.27 (m, 1H, 17-H), 4.53 (q, 1H, 18-H), 4.90−4.00 (m, 4H, 13^1,15^1-CH_2CH_2), 3.88 (q, 2H, 3-CH_2CH_3), 3.61, 3.40, 3.38 (each s, 3H, CO_2CH_3 and 2-, 12-CH_3), 2.80−2.05 (m, 4H, 17-CH_2CH_2), 2.69 (m, 2H, 7-CH_2), 1.94 (s, 3H, 7-CH_3), 1.78 (s, 3H, 18-CH_3), 1.73 (t, 3H, 3-CH_2CH_3), 0.41 (t, 3H, 7-CH_2CH_3), −1.61, −2.82 (each s, 1H, NH); HRMS calcd for $C_{34}H_{40}N_4O_3$ 552.3098, found 552.3097.

Methyl 13^1-Deoxy-20-formyl-7,8-*vic*-dihydroxybacteriomesopheophorbide-*a* (Diastereomeric Mixture, *cis-up* and *cis-down*) (10). Pheophorbide **9** (200 mg) was dissolved in dichloromethane (20 mL). Pyridine (5 drops) along with osmium tetroxide (200 mg)/carbon tetrachloride (2.0 mL) were added, and the reaction mixture was stirred in a sealed flask overnight. The reaction was monitored by analytical TLC and spectrophotometrically. Methylene chloride (100 mL) was added, and H_2S gas was bubbled through the solution for 5 min. The reaction mixture was filtered. The filtrate was evaporated, and the residue was chromatographed over silica column, eluting with 5% methanol/methylene chloride. The slow-moving band was collected. After the solvent was evaporated, the residue was crystallized from CH_2Cl_2/hexane as a fluffy solid: yield 128 mg (60%); mp 180 °C; UV−vis λ_{max} (nm, ϵ) 369 (84 800), 408 (69 800), 531 (26 800), 680 (10 800), and 756 (36 000); ^{1}H NMR δ (ppm) 11.90, 11.70 (each s, 1H, CHO), 8.90, 8.80 (each s, meso H), 8.60 (s, 2H, 2 meso H), 5.10, 5.00, 4.50, and 4.00 [each m, total 12H, 2 × (13^1 and 15^1-CH_2CH_2, 17-H and 18-H)], 3.80 (m, 4H, 2 × CH_2-CH_3), 3.60, 3.50, 3.22, and 3.20 (each s, 3H, ring CH_3), 2.20 and 2.10 (s, 3H, 2 × 7-CH_3), 1.30 (d, 6H, 18-CH_3), 0.90 (m, 4H, 2 × ring B CH_2CH_3), 0.70 (t, 6H, 2 × CH_2CH_3), −0.12, −0.25, −1.40, −1.70 (each s, 1H, NH); HRMS calcd for $C_{35}H_{42}N_4O_5$ 598.3149, found 598.3156; HPLC analysis sovent A (see the text) 9.84 min (broad peak).

13^1-Deoxy-20-formyl-*vic*-dihydroxybacteriochlorin Di-*tert*-butyl Aspartate (Diasteriomeric Mixture, *cis-up* and *cis-down*) (13). The aspartic acid derivative **12** (150 mg) was reacted with osmium tetroxide (150 mg) following the method discussed for the foregoing bacteriochlorin, and the title product was isolated in 70% yield; mp 185 °C; UV−vis λ_{max} (nm, ϵ) 369 (83 600), 408 (68 700), 534 (23 200), 680 (9600), 756 (33 500); ^{1}H NMR (as diastereomers) δ 11.90, 11.80 (each s, 1H, CHO), 8.80, 8.75 (each s, 1H, meso H), 8.60 (s, 2H, 2 meso H), 6.38, 6.10 (each d, 1H, CONH), 5.10−3.60 [m, 14 H, 2 × (13^1,15^1-CH_2CH_2, 17-H, 18-H, CHCO$_2$Bu^t)], 3.30, 3.28 (each s, 3H, ring CH_3), 2.80−2.25 [m, 12H, 2 × ($CH_2CO_2Bu^t$, 17-CH_2CH_2)], 2.10 (s, 6H, 7-CH_3), 1.70−1.50 (12H, d and t merged, 18-CH_3 and 8-CH_2CH_3), 1.38, 1.35, 1.30, 1.25 (each s, 9H, $C(CH_3)_3$], −0.12, −0.20, −1.40, and −1.60 (each s, 1H, NH); HRMS calcd for $C_{46}H_{61}N_5O_5$ 811.4562, found 811.4521; HPCL analysis, solvent B (see the experimental section) 2.96 and 3.91 min.

Methyl 13^1-Deoxy-20-formyl-4-ketobacteriochlorin (11). *vic*-Dihydroxybacteriochlorin **10** (65 mg) was dissolved in sulfuric acid (15 mL), and the reaction mixture was stirred at room temperature under N_2 for 2 h. It was then poured in ice cold water and extracted with methylene chloride (3 × 200 mL). The organic layer was washed with water (4 × 200 mL), aqueous 10% sodium bicarbonate (100 mL), and again with water. The organic layer was separated and dried over anhydrous sodium sulfate. Evaporation of the solvent gave a residue which was crystallized from CH_2Cl_2/hexane as a fine powder: yield 62%; mp 185 °C; UV−vis λ_{max} (nm, ϵ) 414 (94 500), 435 (78 400), 516 (11 200), 676 (7300), 732 (25 700); ^{1}H NMR δ 12.06 (s, 1H, CHO), 9.34 and 8.88 (each s, 1H, meso H), 3.90−5.30 (m, 6H, 13^1- and 15^1-CH_2CH_2, 17-H and 18-H), 3.84 (m, 2H, 3-CH_2CH_3), 3.63 (s, 3H, CO_2CH_3), 3.35, 3.31 (each s, 3H, ring CH_3), 2.00−2.75 (m, 4H, 17-CH_2CH_2), 1.91 (s, 3H, ring 7-CH_3), 2.63 (q, 2H, 7-CH_2CH_3), 1.67 (t, 3H, 7-CH_2CH_3),

1.40 (d, 3H, 18-CH_3), 0.46 (t, 3H, 7-CH_2CH_3), −0.33 and −1.62 (each s, 1H, 2 NH); HRMS calcd for $C_{35}H_{40}N_4O_4$ 580.3044, found 580.3030; HPLC analysis, sovent B (see Experimental Section) 7.92 min.

13¹-Deoxy-20-formyl-4-ketobacteriochlorin Di-*tert*-butyl Aspartate (14). The ketobacteriochlorin **11** (100 mg) was first hydrolyzed to the corresponding carboxylic acid using aqueous lithium hydroxide (100 mg in 2.0 mL water) in a THF/MeOH mixture (30 mL, 2:1) and then reacted with aspartic acid di-*tert*-butyl ester as described for the preparation of bacteriochlorin **6**. The desired compound was obtained in 75% yield (75 mg): mp 185 °C; UV−vis λ_{max} (nm, ϵ) 414 (91 200), 432 (76 200), 516 (12 600), 678 (6900), 735 (25 300); ^{1}H NMR δ 12.10 (s, 1H, CHO), 9.80, 8.80 (each s, 1H, meso H), 6.40 (1H, CONH), 5.50−3.50 [11H, 13¹-,15¹-CH_2CH_2, 17-H, 18-H, 2-CH_2CH_3), $CH(CO_2Bu^t)$], 3.70, 3.65 (each s, 3H, ring CH_3), 2.0−2.8 (m, 6H, 17-CH_2CH_2, $CH_2CO_2Bu^t$), 1.85 [s, 3H (7-CH_3)], 1.70 (t, 3H, 3-CH_2CH_3), 1.45 (d merged with s, 12H, 18-CH_3 and $CO_2C(CH_3)_3$], 1.25 [s, 9H, $CO_2C(CH_3)_3$], 0.50 (t, 3H, 7-CH_2CH_3), −0.40 and −0.70 (each s, 1H, 2NH); HRMS calcd for $C_{46}H_{59}N_5O_7$ 793.4421, found 793.4415; HPLC analysis, solvent B (see the Experimental Section) t_R 7.01 min.

Methods for Photophysical Characterization. The long wavelength absorption (Q-band maximum) of some selected sensitizers in benzene are shown in Table 1. Fluorescence quantum yields were measured on a "per photon basis" relative to tetraphenylporphyrin (TPP) in benzene.[33] The ground state absorbances of the sample solutions were matched at 0.05 (excitation wavelength: 410 nm). Fluorescence emission spectra of the reference solution and the sample solutions were recorded using a Perkin-Elmer LS5 spectrofluorimeter under similar conditions (room temperature, excitation, and emission slits set at 2.5 nm).

Transient Absorption. Triplet−triplet absorption spectra and kinetics were obtained using a custom-built (Kinetics Instruments KI-01) kinetic absorption spectrophotometer coupled to a Q-switched Nd:YAG laser (Continuum Surelite I) for excitation. This instrument uses a PC 486 personal computer equipped with software written to control the experiment, to acquire and manipulate the data, and to perform kinetic analysis. Singlet oxygen quantum yields were determined using a time-resolved method employing a liquid N_2 cooled Ge detector and amplifier combination (ADC 403 HS). These systems have been described previously.[34] An excitation wavelength of 355 nm was employed. Difference triplet−triplet absorption of the compounds were similar in both argon- and air-saturated solutions. Triplet absorption maxima are shown in Table 2, along with the decay rate constant k_0 of the triplet state in argon-saturated solutions. All triplet states were quenched by molecular oxygen with monoexponential decay. Bimolecular quenching rate constants (k_q) of the triplet by molecular oxygen are reported in Table 2.

Singlet Oxygen Yield. Singlet oxygen quantum yields were measured relative to TPP in benzene by monitoring the temporal changes of the near infrared (NIR) luminescence intensities resulting from photoexcitation at 355 nm. All samples yielded NIR luminescences showing a prompt increase in intensity and a slow decaying component resulting from the luminscence of singlet oxygen. Single amplitude L_0 due to singlet oxygen at $t = 0$ was derived from the time-resolved decay and is given by the relationship

$$L_0 = Bk_r\Phi_\Delta{}^\eta AE$$

where k_r is the radiative rate constant for the $^1\Delta_g \rightarrow {}^3\Sigma_g{}^{-1}$ transition of O_2, Φ_Δ is the singlet oxygen quantum yield, B an instrumentation factor, A is the ground state absorbance at λ_{exc}, and E is the energy of the excitation pulse. The quenching efficiency η is defined by

$$\eta = k_q[O_2]/k_0 = k_q[O_2]$$

For all samples investigated, $k_q[O_2] >> k_0$ and η is close to unity. L_0 values were determined from measurements of the NIR luminescense sample solutions and a reference solution (TPP in benzene) under similar experimental conditions. Plots of L_0 of the sample vs L_0 of the reference were linear. From such plot, slop k_{x-r} was derived to calculate the relative singlet oxygen quantum yield according to the relation

$$k_{x-r} = \Phi^x{}_\Delta A^x/\Phi^r{}_\Delta A^r$$

where A^r and A^x are the ground state absorbance of the reference and the sample solutions respectively. Values for the singlet oxygen yields are reported in Table 2.

HSA Binding Experiments. Materials. Human serum albumin prepared from fraction V and dansyl-L-proline (DP) and 5-(dimethylamino)naphthalene-1-sulfonamide (DNSA) were purchased from Sigma Chemical Co. (St. Louis, MO). DP and DNSA were used as site I and site II probes, respectively.

Apparatus. Fluorescence measurements were carried out with a JASCO model FP-777 spectrofluorometer (Tokyo, Japan) using cuvettes of pathlength 10 mm. A bandpass of 10 nm was used for both excitation and emission slits.

Preparation of Control Curve. Control fluorescence intensities of unbound probes were measured at 476 nm with excitation at 340 nm for DP or DPSA in water (1×10^{-6} mol/L). Similarly, control fluorescence intensities of bound probes were measured with the probe (1×10^{-6} mol/L) using relatively large amounts of HSA (2.5×10^{-5} mol/L).

Direct Ultrafiltration. The ultrafiltration experiments were performed in Millipore Ultrafree-CL Filter Units, 30 000 NMWL low-binding PLTK membrane (Bedford, MA). In our experiments, the bacteriochlorins and HSA did not pass through the filter unit membranes. On the other hand, adsorption of DP on the membranes was negligible. HSA−DP complex solution was filtered with or without the bacteriochlorin derivatives. Primary concentration of HSA was fixed at 5×10^{-7} mol/L, the concentration of the bacteriochlorin derivatives was also fixed at 1×10^{-6} mol/L, and the concentration of DP was varied from 2×10^{-6} to 6×10^{-7} mol/L. The mixed solution (2 mL) was incubated at 4 °C, pH 7.0, for 3 h in the dark and centrifuged at 3000 rpm for 2 min. The volume of filtered solution was less than 15% (0.3 mL) of the primary solution. The filtered solution (0.2 mL) was then mixed with HSA (final concentration 2.5×10^{-5} mol/L, 1.8 mL) and incubated at 4 °C, pH 7.0, for 1 h in dark. Fluorescence from DP (emission 476 nm, excitation 340 nm) was measured with the spectrofluorometer. The concentration of filtered DP was calculated from the standard curve.

Fluorescence Titrations. Titrations of the binding site probe (DP) against HSA with photosensitizers were performed as follows: Concentrations of HSA and each photosensitizer were fixed at 1×10^{-6} mol/L. On the other hand, concentrations of the binding site probes were varied from 4×10^{-7} to 2×10^{-6} mol/L. Fluorescent intensities at 476 nm with excitation at 340 nm were measured respectively after incubating at 4 °C, pH 7.0, for 4 h in dark. The concentration of HSA bound DP was calculated with the standard curve. The data sets were analyzed with the Origin (version 4.0) program on an IBM-PC computer.

Titrations of the binding site probes (DNSA and DP) against HSA with bacteriochlorins were performed as follows: Concentrations of HSA and each bacteriochlorins were kept constant at 1×10^{-6} mol/L, respectively. On the other hand, concentrations of the binding site probes were changed from 4×10^{-7} to 2×10^{-6} mol/L. Fluorescent intencities at 472 nm in the case of DNSA or at 476 nm in the case of DP were measured with excitation at 340 nm were measured.

Control fluorescence intensities of unbound probes were measured at 472 nm in the case of DNSA and at 476 nm in the case of DP by exciting the peak at 340 nm for each probe in water (1×10^{-6} mol/L).

Titration of Binding Site Probes against HSA with Various Bacteriochlorins. Spectrofluorimetric titrations were performed to determine the concentration of each bound binding site probe (DNSA or DP) with or without each drug. The binding site probes reported by Sudlow *et al.*[28,29] are known to increase their fluorescence intensities when they bind with

HSA. Therefore, the binding parameters can be calculated by the following formulas with spectrofluorimetric titrations.

The concentration of the bound drug (C_b) can be described as follows:

$$C_b = C_t(Q_{obs} - Q_u)/(Q_b - Q_u) \quad (1)$$

where, C_t is the total concentration of the drug, Q_{obs} is the observed quantum yield of the drug (bound and unbound), Q_u is the quantum yield of unbound drug, and Q_b is the quantum yield of the bound drug. Formula 1 can be derived from following formulas.

$$I = 2.303\epsilon QlI_{ex}C \quad (2)$$

$$I_{obs} = I_u + I_b \quad (3)$$

$$C_t = C_b + C_u \quad (4)$$

In formula 2, I is the fluorescence intensity, ϵ is the molar absorptivity, Q is the quantum yield, l is the pathlength of the cuvette, I_{ex} is the intensity of excitation light, C is the concentration. In formula 3, I_{obs} is the fluorescence intensity of the drug (bound and unbound), I_u is the fluorescence intensity of the unbound drug, I_b is the fluorescence intensity of the bound drug. In formula 4, C_t is the total concentration of the drug, C_b is the concentration of bound drug, and C_u is the concentration of the unbound drug.

With formulas 2, 3, and 4, formula 1 can be transformed into

$$C_b = C_{tx}(I_{obs}/C_t - I_u/C_u)/(I_b/C_b - I_u/C_u) \quad (5)$$

If the drug binds specifically with HSA, the binding parameters can be calculated as follows:

$$r = (KC_u)/(1 + KC_u) \quad (6)$$

$$r = C_b/P_t \quad (7)$$

where, r is the number of drug molecules binding with a molecule of HSA, K is the binding constant, and P_t is the total concentration of HSA. The binding parameters can be estimated by nonlinear least-squares curve fitting (NLSCF) method.

In the case of competitive inhibition (between probes and drugs), the binding properties can be expressed as follows:

$$r_A = \frac{K_A A_u}{1 + K_A A_u + K_B B_u} \quad (8)$$

In formula 8, K_A is the binding constant of the probe, K_B is that of the drug. r_A is the number of probes binding with each HSA molecule. A_u is the concentration of unbound probe, and B_u is the concentration of unbound drug. B_u is unknown but can be derived as follows

$$B_t = B_u + r_B P_t \quad (9)$$

where, r_B is the number of drug molecules binding with each HSA molecule. r_B can be calculated in similar way as obtaining r_A (see formula 8). Thus,

$$r_B = \frac{K_B B_U}{1 + K_B B_u + K_A A_u} \quad (10)$$

From formula 9, r_B can be converted as follows:

$$r_B = \frac{B_t - B_u}{P_t} \quad (11)$$

From formulas 10 and 11, B_u can be expressed as a function of A_u while K_A, K_B, P_t, and B_t are constants. Thus, using caluculated B_u, r_A can be expressed as a function of A_u with constants K_B, K_B, P_t, and B_t as follows:

$$r_A = \frac{2K_A A_u}{1 + K_A A_u + B_t K_B - P_t K_B \pm b^2 - 4ac} \quad (12)$$

$$a = K_B,\ b = 1 + K_A A_u + P_t K_B - B_t K_B$$

In this study, K_A was calculated independently using formula 8. Thus, K_B is the only unknown constant in formula 12. To calculate K_B, the NLSCF method with Origin (V 4.1 for Windows) was used.

In those cases where drugs can also bind with an independent binding site other than the competitive site, formulas 10 and 12 were modified as follows

$$r_B = \frac{K_1 B_u}{1 + K_A A_u + K_1 B_u} + \frac{K_2 B_u}{1 + K_2 B_u} \quad (13)$$

$$r_A = f(A_u, K_A, K_1, K_2, P_t, B_t) \quad (14)$$

where K_1 is the binding constant between the drug and the competitive site and K_2 is the binding constant between the drug and the noncompetitive (independent) binding site. In some cases, mutual dependency between K_1 and K_2 was observed. However, the dependency could be waived by adopting multiple data sets from various concentration of the drug and/or HSA.

Acknowledgment. We gratefully acknowledge the support from the Mallinckrodt Medical Inc., St. Louis, the National Institutes of Health (CA 55791; HL 22252), and the Oncologic Foundation of Buffalo. Mass spectrometric analyses were performed at the mass spectrometry facility, Michigan State University, East Lansing. We express our appreciation to Dr. B. Paul and Mr. B. F. Mayer, Department of Experimental Therapeutics (core grant CA16050) for isolating methylpheophorbide-*a* from *Spirulina pacifica*. C.J.M. thanks Professor J. A. Shelnutt (Sandia National Laboratories, New Mexico) for financial support from U.S. Department of Energy Grant DE-ACO4-94AL85000.

References

(1) (a) Dougherty, T. J.; Marcus, S. C. Photodynamic therapy. *Eur. J. Cancer* **1992**, *28A* (10), 1734−1742. (b) Gomer, C. J.; Rucker, N.; Ferrario, A.; Wang, S. Properties and application of photodynamic therapy. *Radiat. Res.* **1989**, *120*, 1−18.

(2) Henderson, B. W.; Dougherty, T. J. How does photodynamic therapy work? *Photochem. Photobiol.* **1992**, *55*, 145−157.

(3) Dougherty, T. J.; Potter, W. R.; Bellnier, D. A. Photodynamic therapy for the treatment of cancer: current status and advances. In *Photodynamic Therapy of Neoplastic Disease*; Kessel, D., Ed.; CRC Press: Boca Raton, 1990; Vol. 1, pp 1−19.

(4) Weishaupt, K. R.; Gomer, C. J.; Dougherty, T. J. Energetics and efficiency of photoinactivation of murine tumor cells containing hematoporphyrin. *Cancer Res.* **1976**, *36*, 2326−2330.

(5) (a) Pandey, R. K.; Smith, K. M.; Dougherty, T. J. Porphyrin dimers as photosensitizers in photodynamic therapy. *J. Med. Chem.* **1990**, *33*, 2032−2038. (b) Pandey, R. K.; Shiau, F. Y.; Medforth, C. J.; Dougherty, T. J.; Smith, K. M. Efficient synthesis of porphyrin dimers with carbon-carbon linkages. *Tetrahedron Lett.* **1990**, *31*, 789−792. (c) Pandey, R. K.; Dougherty, T. J.; Smith, K. M. Synthesis of hematoporphyrin dimers and trimers with ether linkages. *Tetrahedron Lett.* **1988**, *37*, 4657−4660. (d) Pandey, R. K.; Shiau, F. Y.; Medforth, C. J.; Dougherty, T. J.; Smith, K. M. Syntheses, stability and tumoricidal activity of porphyrin dimers and trimers with ether linkages. *Tetrahedron Lett.* **1990**, *31*, 7399−7402. (e) Berenbaum, M. C.; Bonnett, R.; Scourides, P. A. *In vivo* biological activity of the components of hematoporphyrin derivative. *Br. J. Cancer* **1982**, *45*, 571−581. (f) Byrne, C. J.; Marshallsay, L. V.; Ward, A. D. *J. Photochem. Photobiol. B: Biol.* **1990**, *6*, 13. (g) Morris, I. K.; Ward, A. D. The synthesis of dihematoporphyrin ether and related porphyrin dimers. *Tetrahedron Lett.* **1988**, *29*, 2501−2504. (h) Pandey, R. K.; Shiau, F. Y.; Dougherty, T. J.; Smith, K. M. Regioselective syntheses of ether linked porphyrin dimers and trimers related to Photofrin-II. *Tetrahedron* **1991**, *47*, 9571−9584.

(6) (a) Pandey, R. K.; Dougherty, T. J. Syntheses and photosensitizing activity of porphyrin joined with ester linkages. *Cancer Res.* **1989**, *49*, 2042−2047. (b) Kessel, D.; Thompson, P.; Musselman, B.; Chang, C. K. Probing the structure and stability of the tumor localizing derivative of hematoporphyroin by reduction with $LiAlH_4$. *Cancer Res.* **1987**, *47*, 4642−4655.

(7) (a) Pandey, R. K.; Siegel, M. M.; Tsao, R.; McReynolds, J. H.; Dougherty, T. J. Fast atom bombardment mass spectral analyses of Photofrin II and its synthetic analogues. *Biomed. Environ. Mass Spectrom.* **1990**, *19*, 405−414. (b) Musselman, B.; Kessel, D.; Chang, C. K. Fast atom bombardment mass spectrometry of high-molecular weight fraction of porphyrin base photodynamic therapy drugs. *Biomed. Environ. Mass Spectrom.* **1988**, *15*, 257−263.

(8) Pandey, R. K.; Zheng, G.; Lee, D. A.; Dougherty, T. J.; Smith, K. M. Comparative *in vivo* sensitizing efficacy of porphyrin and chlorin dimers joined with ester, ether and carbon-carbon or amide bonds. *J. Mol. Recogn.* **1996**, *9*, 118−122.

(9) (a) Floch, S. T.; Wilson, B. C.; Paterson, M. Monte Carlo modeling of light propagation in highly scaterring tissues: Comparision with measurements in Photofrin. *IEEE Trans. Biomed. Eng.* **1989**, *36*, 1169−1173. (b) Bonnett, R.; Berenbaum, M. Porphyrins as photosensitizers in Photosensitizing compounds: Their chemistry, biology and clinical use. *Ciba Foundation Symposium 146*; John Wiley and Sons: New York, 1989; pp 40−59.

(10) For reviews, see: (a) Sessler, J. L.; Hemmi, G.; Mody, T. D.; Murai, T.; Burrell, A.; Young, S. W. Texaphyrins: synthesis and applications. *Acc. Chem. Res.* **1994**, *27*, 43−53. (b) Bonnett, R. Potosensitizers of the porphyrin and phthalocyanine series for photodynamic therapy. *Chem. Soc. Rev.* **1995**, *24*, 19−33. (c) Pandey, R. K.; Majchrzycki, D. F.; Dougherty, T. J.; Smith, K. M. Chemistry of Photofrin II and some new photosensitizers. *Proc. SPIE* **1989**, *1065*, 164−174.

(11) Beems, E. M.; Dubbelman, T. M. A. R.; Lugtenburg, J.; Best, J. A. V.; Smeets, M. F. M. A.; Boegheim, J. P. J. Photosensitizing properties of bacteriochlorophyll-a and bacteriochlorin-a. *Photochem. Photobiol.* **1987**, *46*, 639−643.

(12) Henderson, B. W.; Sumlin, A. B.; Owczarczak, B. L.; Dougherty, T. Bacteriochlorophyll-a as photosensitizer for photodynamic treatment of transplantable murine tumors. *J. Photochem. Photobiol.* **1991**, *10*, 303−313.

(13) (a) Chang, C. K.; Sotiriou, C.; Wu, W. Differentiation of bacteriochlorin and isobacteriochlorin formation by metallation. High yield synthesis of porphyrindiones *via* OsO_4 oxidation. *J. Chem. Soc., Chem. Commun.* **1986**, 1213−1214. (b) Chang, C. K.; Sotiriou, Migratory aptitudes in pinacol rearrangement of *vic*-dihydroxybacteriochlorins. *J. Heterocycl. Chem.* **1995**, *22*, 1739−1742.

(14) Pandey, R. K.; Shiau, F. Y.; Isaac, M.; Ramaprasad, S.; Dougherty, T. J.; Smith, K. M. Substituent effects in tetrapyrrole subunit reactivity and pinacol-pinacolone rearrangements.*Vic*-dihydroxychlorins and *vic*-dihydroxybacteriochlorins. *Tetrahedron Lett.* **1992**, *33*, 7815−7818.

(15) Kozyrev, A. N.; Pandey, R. K.; Medforth, C. J.; Zheng, G.; Dougherty, T. J.; Smith, K. M. Synthesis and unusual spectroscopic properties of novel ketobacteriochlorins. *Tetrahedron Lett.* **1996**, *37*, 747−750.

(16) Pandey, R. K.; Shiau, F. Y.; Sumlin, A. B.; Dougherty, T. J.; Smith, K. M. Syntheses of new bacteriochlorins and their antitumor activity. *Bioorg. Med. Chem. Lett.* **1994**, *4*, 1263−1267.

(17) Pandey, R. K.; Isaac M.; MacDonald, I.; Senge, M. O.; Dougherty, T. J.; Smith, K. M. Pinacol-pinacolone rearrangements in *vic*-dihydroxychlorins and bacteriochlorins: Effect of substituents at the peripheral positions. *J. Org. Chem.* **1997**, *62*, 1463−1472.

(18) Kozyrev, A. N.; Dougherty, T. J.; Pandey, R. K. Effect of substituents in OsO_4 reactions of metallochlorins. Regioselective synthesis of isobacteriochlorins and bacteriochlorins, *Tetrahedron Lett.* **1996**, *37*, 3781−3784.

(19) Dougherty, T. J.; Boyle, D. G.; Weishaupt, K. R.; Bellnier, D. A.; Wityk, K. E., Photoradiation therapy-clinical and drug advances. *Adv. Exp. Med. Biol.* **1984**, *170*, 301−314.

(20) (a) Selman, S. H.; Birnbaum, M. K.; Klauing, J. E.; Goldbart, P. J.; Keck, P. W.; Britton, S. L. Blood flow in transplantable bladder tumors treated with hematoporphyrin derivative and light. *Cancer Res.* **1984**, *44*, 1924−1927. (b) Henderson, B. W.; Fingar, V. H. Relationship of tumor hypoxia and response to photodynamic treatment in an experimental mouse tumor. *Cancer Res.* **1987**, *47*, 3110−3114.

(21) Moan, J.; Rimington, C.; Western, A. The binding of dihematoporphyrin ether (Photofrin II) to human serum albumin. *Clin. Chim. Acta* **1985**, *145*, 227−236, and references therein.

(22) He, X. M.; Carter, D. C. Atomic structure and Chemistry of human serum albumin. *Nature* **1992**, *358*, 209−215.

(23) Pandey, R. K.; Sumlin, A. B.; Constantine, S.; Aoudia, M.; Potter, W. R.; Bellnier, D. A.; Henderson, B. W.; Rodgers, M. A.; Smith, K. M.; Dougherty, T. J. Alkyl ether analogues of chlorophyll-a derivatives: Part I. Synthesis, photophysical properties and photodynamic efficacy. *Photochem. Photobiol.* **1996**, *64*, 194−204.

(24) Tsuchida, T.; Zheng, G.; Pandey, R. K.; Potter, W. R.; Bellnier, D. A.; Henderson, B. W.; Kato, H.; Dougherty, T. J. Correlation between site II specific human serum albumin (HSA) binding affinity and in vivo photosensitizing efficacy of some Photofrin components. *Photochem. Photobiol.*, in press.

(25) Smith, K. M.; Goff, D. A.; Simpson, D. J. Meso substutution of chlorophyll derivatives: direct route for transformation of bacteriopheophorbides d into bacteriopheophorbide c. *J. Am. Chem. Soc.* **1985**, *107*, 4941−4954.

(26) Smith, K. M. *The Porphyrins and Metalloporphyrins*; Smith, K. M., Ed.; Elesvier Scientific Publication: Amsterdam, 1975.

(27) Jeandon, C.; Ocampo, R.; Callot, H. J. Improved preparation of deoxyphyllo- erythreoetio porphyrin (DPEP) and its 15-methyl derivative from chlorophyll-a. *Tetrahedron Lett.* **1993**, 34, 1791−1794.

(28) Sudlow, G.; Birkett, D. J.; Wade, D. N. The characterization of two specific drug binding sites on human serum albumin. *Mol. Pharmacol.* **1975**, *11*, 824−832.

(29) Sudlow, G.; Birkett, D. J.; Wade, D. N. Further characterization of specific drug binding sites on human serum albumin. *Mol. Pharmacol.* **1976**, *12*, 1052−1061.

(30) Gibson, S. L.; Hilf, R. Photosensitization of mitochondrial cytochrome-c oxidised by hematoporphyrin derivatives. *Cancer Res.* **1993**, *43*, 4191−4197.

(31) Verma, A.; Nye, J. S.; Suyder, S. H. Porphyrins are endogenous ligands for the mitochondrial (peripheral type) benzodiazepine receptor. *Proc. Natl. Acad. Sci. U.S.A.* **1992**, *84*, 2256−2260.

(32) Norman Smith, Ph.D. Thesis, Department of Chemistry, University of California, Davis, 1991.

(33) Harriman, A. Luminenscence of porphyrins and metalloporphyrins. *J. Chem. Soc., Faraday Trans. 1* **1980**, *76*, 1978−1985.

(34) Zheng, X.; Rodgers, M. A. J. Energy and electron transfer reactions of the MLCT state of ruthenium tris(bipyridyl) with molecular oxygen: a laser flash photolysis study. *J. Phys. Chem.* **1996**, *99*, 12797−12803.

JM9702894